

Roof Stability Evaluation of Bedded Rock Salt Cavern Used as Underground Gas Storage

Tongtao Wang, Xiangzhen Yan, Xiujuan Yang and Tingting Jiang
College of Pipeline and Civil Engineering, China University of Petroleum,
Qingdao 266580, Shandong, China

Abstract: The cusp catastrophe model is proposed in the study to evaluate the roof stability factor of natural gas storage cavern in bedded rock salt, which can overcome the shortages of traditional Strength Reduction Finite Element (or difference) Method (SR FEM) that the failure criteria can not be precisely given. The proposed model can greatly improve the calculating precision and has clear physical and mathematical meanings. The numerical simulations of generic natural gas storage caverns in bedded rock salt located in Jiangsu province of China are carried out based on the proposed model to evaluate the stability factor of cavern roof. In addition, parameters are studied to investigate the stability factors as functions of the buried depth, roof span, roof salt thickness and roof salt Young's modulus, overlying non-salt thickness, overlying non-salt Young's modulus and gas pressure, etc. The examples show that the proposed model is precise and correct, which can meet the actual engineering demands. The stability factor of cavern roof is equidirectional with the increase of roof salt thickness, roof salt stiffness, overlying non-salt thickness, overlying non-salt stiffness and gas pressure, but reverse to the increase of buried depth and roof span. Our methods provide a new way to evaluate the roof stability factor of natural gas storage cavern in bedded rock salt.

Keywords: Bedded rock salt cavern, cusp catastrophe model, numerical simulation, roof stability, strength reduction

INTRODUCTION

Bedded rock salt beds are widespread and used more than salt domes as oil/ gas storage facility hosts in China. For the relatively thin nature of salt beds and the local presence of other sedimentary rock formations, i.e., shale, anhydrite and glauberite (Liang *et al.*, 2007; Wang *et al.*, 2010a, b; Wang *et al.*, 2011a, b; Yang *et al.*, 2008), the problems present unique to bedded rock salt storage that are generally nonexistent in caverns located in salt domes. In salt dome, storage cavern is typically cylindrically shaped. The dimension of its height is significantly bigger than that of its diameter, resulting in a nicely domed roof, which is favorable from a mechanical stability standpoint. Whereas the height of a bedded rock salt cavern depends on the thickness of the rock salt bed and is usually much less than that of a cavern located in salt dome. This forces the ratio of diameter and height of a bedded rock salt cavern to be much greater than that of salt dome cavern to obtain sufficient storage volume. The bedded rock salt cavern configuration is less desirable from a rock mechanics standpoint because of the potentially large roof spans that must be supported by the geologic formation. In addition, the favorable domed roof is impossible to obtain for the relatively thin nature of the salt beds. Therefore, how to design the cavern roof and

predict the stability of natural gas storage cavern in bedded rock salt are always hot issues in the engineering field (Liang *et al.*, 2007; Vries, 2006).

The stability evaluations of nonlinear material structures, such as soil slopes, coal laneways and mine pits, etc., have already formed a series of constructive engineering theories and methods, including the most widely used SR FEM (Manzari and Nour, 2000; Dawson *et al.*, 2000; Huang and Jia, 2009; Joanna *et al.*, 2010). The SR FEM not only gives the overall stability safety factor of structures, but also provides the detailed information of each node locations (e.g., stress, strain and deformation). In SR FEM, the SR factor increases gradually until the structure reaches the global failure. Then, the corresponding SR factor can be considered as the critical stability factor of the structure. Generally, the critical failure of non-linear material structure can be denoted by 3 criterions in the numerical simulations (Dawson *et al.*, 2000; Huang and Jia, 2009; Joanna *et al.*, 2010; Matsui and San, 1992), namely:

- Non-convergence of iterations
- Plastic zone exceeding the limit
- Relations between deformation (or stress) and SR factor

However, these criterions all have their shortages in the actual operations. For examples, the non-convergence of iterations has indefinite physical meaning and the results of available literatures (Sanavia, 2009) showed that the plastic zone had already pierced while the structure was still stable. Moreover, both the non-convergence and plastic zone are greatly affected by the quality and number of mesh, which have a random city with operator's capability. Nevertheless, for the complicated properties and post failure of nonlinear material, the deformation (or stress) of structure does not have the only one relevant relationship with SR factor when different locations are chosen as referenced calculating points. It makes the critical stability factor obtained by SR FEM is inaccurate and influenced greatly by human factors.

As cusp catastrophe theory, structure dissipation and nonlinear dynamics, etc., (Leynaud and Sultan, 2010; Fu and Chen, 2008; Kemal *et al.*, 2007; Yang *et al.*, 2010; Bornyakov *et al.*, 2008; Qin *et al.*, 2001; Zhou *et al.*, 2008) have been successfully introduced into the stability evaluation of nonlinear material structure, which also provide powerful tools for evaluating the stability of bedded rock salt cavern gas storages. Thom (1989) first proposed the cusp catastrophe theory, which was mainly used to depict numerous sudden discontinuous change phenomena in nature and predict the critical condition of structure mutation. The instability of salt cavern roof is caused by the overburden pressure and far field in-situ stress. It is a typical energy accumulation and release process, viz., when the stresses and deformations of cavern roof reach certain critical values, the accumulated stresses and strains energy release instantly and the failure of cavern roof takes place. Therefore, the instability of cavern roof can be considered as the process that the deformations of cavern roof change from continuous state to system catastrophe state, which is a typical non-linear cusp catastrophe problem.

In the study, the cusp catastrophe model is proposed in the traditional SR FEM to evaluate the roof stability factor of bedded rock salt cavern used as natural gas storage, which could overcome the shortages that the failure criterions can not be given precisely and greatly improve the accuracy of stability factor obtained by SR FEM. Furthermore, the natural gas storage caverns in bedded rock salt located in Jiangsu province of China are simulated as examples. The stability factor of cavern roof is given for different work conditions. The effects of parameters on the stability factor of cavern roof are also studied.

CUSP CATASTROPHE MODEL

SR FEM: The stability factor evaluation of non-linear material (such as soil, rock, coal, etc.) structure by SR FEM has been applied successfully by many researchers (Zienkiewicz *et al.*, 1975; Donald and Giam, 1988; Ugai, 1989; Matsui and San, 1992; Ugai and Leshchinsky, 1995; Dawson *et al.*, 1999; Griffiths and Lane, 1999; Manzari and Nour, 2000; Diederichs *et al.*, 2007; Wei and Cheng, 2009). This method allows finding the safety factor of a structure by initiating a systematic reduction sequence for the available shear strength parameters C' and ϕ' to just cause the structure to fail, shown in Fig. 1. The reduction values of shear strength parameters C' and ϕ' are defined as (Dawson *et al.*, 2000; Huang and Jia, 2009):

$$C' = C / F_i \quad (1)$$

$$\phi' = \arctan(\tan \phi / F_i) \quad (2)$$

where, C and ϕ are the cohesion and friction angle of non-linear material respectively; C' and ϕ' are the reduced cohesion and friction angle respectively; F_i stands for SR factor.

As above descriptions, the SR FEM is used to obtain the stability factor of non-linear material structure, e.g., salt cavern gas storage, with some limitations and low accuracy. In order to overcome these shortages, the relations between the max. vertical deformations of cavern roof and SR factors F_i are built up in the study. Then, the cusp catastrophe model is involved to obtain the accurate stability factor of cavern roof from the relations. The detailed procedures are depicted as follows.

Fundamental theory of cusp catastrophe:

Considering the mutation of vertical deformation is the index of cavern roof instability, the relations between the vertical deformations of cavern roof and SR factors are:

$$z = z(F) \quad (3)$$

As the standard forms of potential function is a fourth-order polynomial formula, which can be obtained by the derivative of (3). Therefore, the fifth-order polynomial formula between the max. vertical deformations and SR factors can be expressed as

$$z = a_0 + a_1 F + a_2 F^2 + a_3 F^3 + a_4 F^4 + a_5 F^5 \quad (4)$$

where, z is the max. vertical deformation of cavern roof (m). a_0, a_1, a_2, a_3, a_4 and a_5 are undetermined constants.

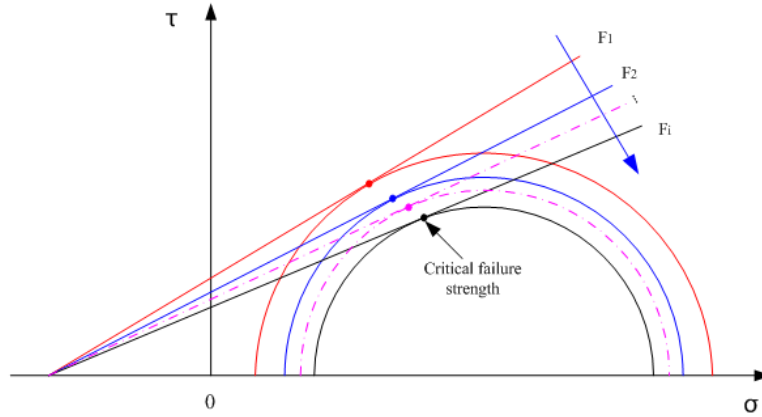


Fig. 1: Diagram of salt damage strength in the numerical simulations by SR FEM

The potential function of vertical deformation can be determined by the first derivative of (4):

$$V = a_1 + 2a_2F + 3a_3F^2 + 4a_4F^3 + 5a_5F^4 \quad (5)$$

The standard form of the potential function can be written as (Qin *et al.*, 2001; Xu and Pen, 2004):

$$V = \frac{1}{4}r^4 + \frac{1}{2}ur^2 + vr \quad (6)$$

where, $u = b_2 / \sqrt{b_3}$, $v = b_1 / \sqrt[4]{4b_3}$, $b_1 = -20a_5q^2 - 6a_3q + 2a_2$, $b_2 = 30a_5q^2 - 12a_5q + 3a_3$, $b_3 = 5a_5$, $q = a_4 / 5a_5$. V is the potential function of vertical deformation. r is the state variable. u, v are the control variables.

Therefore, the balance surface equation of critical deformation mutation can be obtained by setting the first derivative of (6) equal to 0, expressed as:

$$r^3 + ur + v = 0 \quad (7)$$

According to (7), the geometric figure of the critical deformation mutation points is a smooth surface with wrinkle, as shown in Fig. 2. It consists of up-leaf, middle-leaf and low-leaf. The up-leaf and low-leaf are stable, whereas the middle-leaf is unstable. All points on the surface (r, u, v) are referred to the balance points of the potential function V . The equation of singular points can be expressed as:

$$\frac{\partial^2 V}{\partial r^2} = 3r^2 + u = 0 \quad (8)$$

If the singularity points are projected onto the control surface (u, v) , the branch points (Fig. 2) can be obtained by (7) and (8), written as:

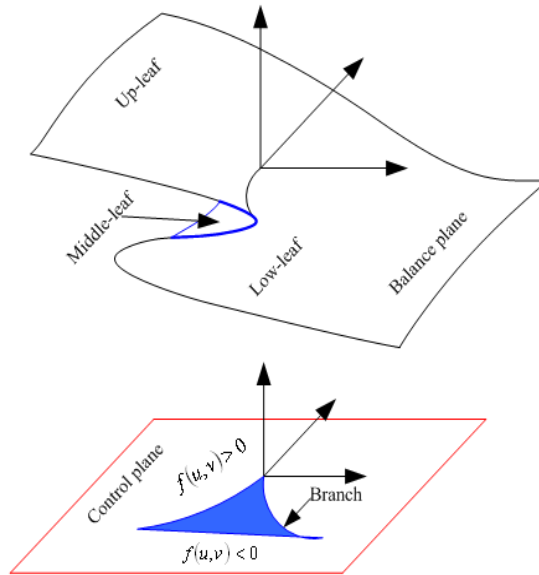


Fig. 2: Balance curve surface and bifurcation set of cusp catastrophe model

$$f(u, v) = 4u^3 + 27v^2 \quad (9)$$

Changes in the control variables u and v basically cause stable changes in the state variable r . Only when the control points (u, v) jump over the branches, will a discontinuous catastrophe occur. The points located at the 2 branches are singularity points of the system (critical stability points of the structure), i.e., catastrophe points. (9) is the set of catastrophe points, which can be used to predict the stability of cavern roof, namely:

- If $f(u, v) > 0$, then the cavern roof is in a stability state

- If $f(u,v) = 0$, then the cavern roof is in a critical stability state
- If $f(u,v) < 0$, then the cavern roof is in a instability state

Stability factor evaluation of salt cavern roof: The main failure types of rock salt in the salt cavern roof are shear and compression failures. Therefore, the Mohr-Coulomb criterion considering both shear and compression a failure of material is adopted in the numerical simulations. The Mohr-Coulomb criterion of shear failure is:

$$f_s = \sigma_1 - \sigma_3 N_\varphi + 2C\sqrt{N_\varphi} = 0 \quad (10)$$

where,

$$N_\varphi = \frac{1 + \sin \varphi}{1 - \sin \varphi} \quad (11)$$

The Mohr-Coulomb criterion of compression failure is:

$$f_t = \sigma_3 - \sigma_t = 0 \quad (12)$$

where, σ_t is the compression strength and its max. value is smaller than $C / \tan \varphi$.

According to above analysis, the whole procedure that the stability factor of salt cavern roof is obtained by SR FEM and cusp catastrophe model can be divided into the following 5 steps, namely:

- Build up the numerical simulation model. According to the cavern dimensions and properties of rock salt and non-salt, the 3D numerical model of bedded rock salt cavern gas storage is established by Flac^{3D} software
- Obtain the initial deformation distribution of salt cavern by numerical simulation with the SR factor of 1.0
- Increase the SR factor F_i gradually (Fig. 1) and substitute the corresponding reduced cohesion and friction into the numerical model
- Obtain the corresponding max. vertical deformations of the cavern roof when the SR factors evaluate differently. The fifth-order polynomial formula of deformations and SR factors are regressed subsequently
- Substitute the calculated parameters into (6) and the control variables u and v are obtained.

According to (9), the stability state of bedded rock salt cavern roof can be predicted

Repeat above procedure until $f(u,v) < 0$. Then, the critical stability factor of cavern roof lies between the SR factor at which $f(u,v) < 0$ and the immediately previous one. The procedure described hereby can precisely predict the stability factor within one loop and can be easily implemented in a computing code.

RESULTS AND DISCUSSION

In order to validate the advantage and accuracy of the cusp catastrophe model proposed in the study, a generic natural gas storage cavern in bedded rock salt located in southeastern China is simulated as an example. The buried depth of objective formation where the salt cavern locates is about 1000 m below ground level. Three non-salt layers are presented in the objective formation and their thicknesses are 4.5, 2.4 and 3.2 m, respectively presenting from roof to bottom. The cavern radius modeled is enlarged near the lower non-salt layer and reduced at the upper non-salt layer, as shown in Fig. 3. Both of these features are common for solution-mined caverns in bedded rock salt formations and provide a realistic cavern shape for evaluation. The total height and max. diameters of cavern are 96 and 58 m, respectively. Part of the upper formation is equal to the vertical principal stress σ_v to make the numerical simulations convenient and efficient. The following boundary conditions are applied: the bottom boundary has zero displacement boundary, viz., the relative horizontal and vertical displacements of the model bottom are all zero under all conditions; both sides of the vertical direction have horizontal zero displacement boundaries. The basic properties of the salt, non-salt and mudstone are listed in Table 1. The numerical simulations investigate several design parameters, including buried depth, cavern roof span, roof salt thickness, roof salt stiffness, overlying non-salt thickness, overlying non-salt stiffness and gas pressure. To assess the effects of the parameters on the stability factors of cavern roof, different conditions are simulated in the numerical calculations, as shown in Table 2.

SR FEM and cusp catastrophe model study cavern roof spans as the examples to illustrate the detailed procedure that the stability factors of cavern roof are obtained. The parameters of the numerical simulations are evaluated as cases 1-7 (Table 2). By increasing SR factors gradually, a series of reduced strength parameters of rock salt and non-salt are obtained. Then, the vertical deformation contours of cavern can be

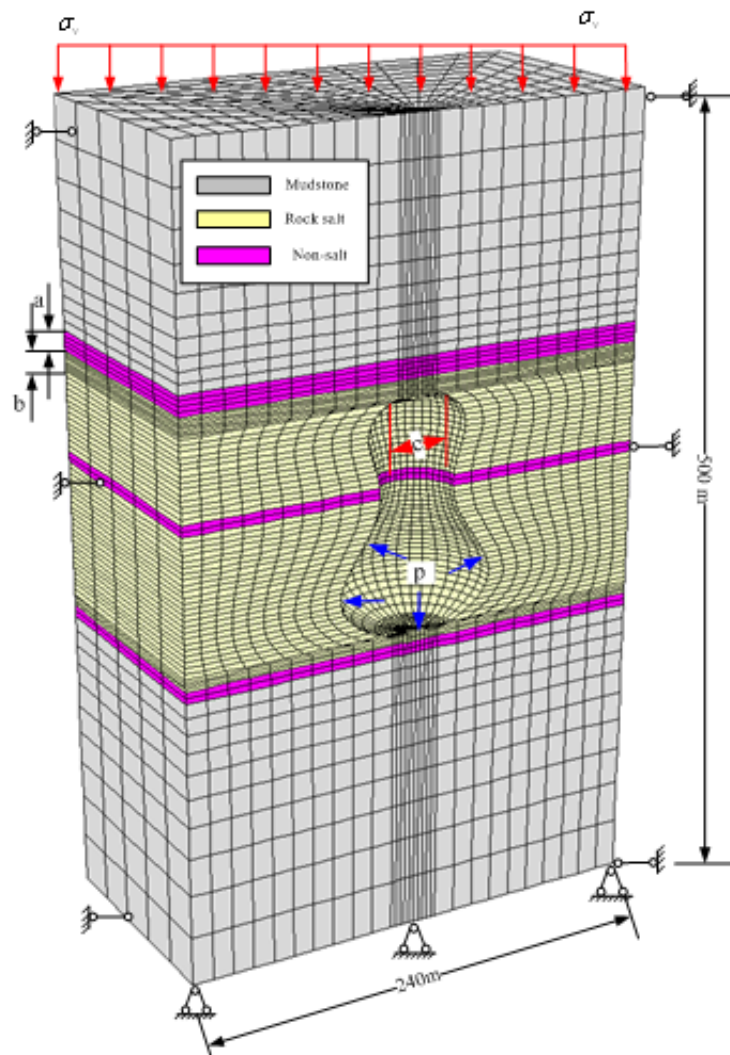


Fig. 3: 3D numerical model of gas storage cavern in bedded rock salt and boundary conditions. a, b are thicknesses of overlying non-salt layer and roof salt, respectively; c is the cavern roof span; σ_v is the self-weight of the upper strata; p is the internal pressure

Table 1: Mechanical property parameters of bedded rock salt

| Geologic unit | Density (Kg/m ³) | Young's modulus (GPa) | Poisson ratio | Cohesion (MPa) | Friction angle (°) | Tensile strength (MPa) |
|---------------|------------------------------|-----------------------|---------------|----------------|--------------------|------------------------|
| Mudstone | 2800 | 10 | 0.27 | 1.0 | 35 | 1 |
| Salt | 2200 | 18 | 0.3 | 1.0 | 45 | 1 |
| Non-salt | 2400 | 4 | 0.3 | 0.5 | 30 | 0.5 |

calculated from numerical simulations (Fig. 4). Figure 4 shows the vertical deformation of cavern with no. 2 calculating condition (Table 2) when SF factors are assigned as 1.0, 1.5, 2.0 and 2.5, respectively. As shown in Fig. 4, the vertical deformation of cavern roof increases as the increasing SR factor for the load carrying capacity of cavern roof decreasing. However, the deformations change continuously indicating the

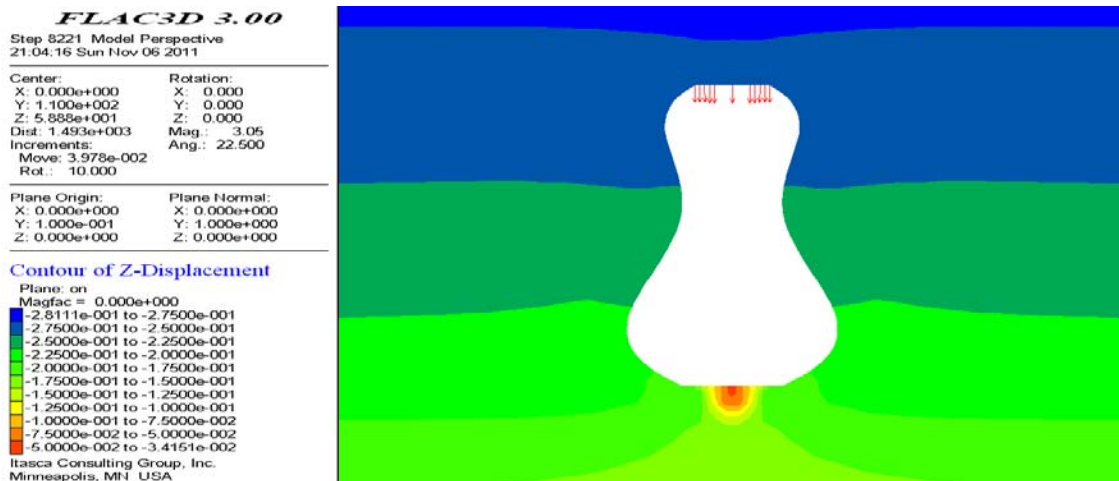
cavern roof is still stable. The max. deformation appears at the center of cavern roof. Therefore, it is selected as the study target to obtain the stability factor of cavern roof.

Similarly, the corresponding max. deformations of cavern roof can be calculated when the SR factors are evaluated as different values. Then, we can obtain the fifth-order polynomial between the max. vertical

Table 2: Cases of calculating conditions

| No. | Roof span (m) | Roof salt thickness (m) | Roof salt Young's modulus (GPa) | Overlying non-salt thickness (m) | Overlying non-salt Young's modulus (GPa) | Gas pressure (MPa) |
|-----|---------------|-------------------------|---------------------------------|----------------------------------|--|--------------------|
| 1 | 5 | 10 | 18 | 4.5 | 4 | 7 |
| 2 | 10 | | | | | |
| 3 | 15 | | | | | |
| 4 | 20 | | | | | |
| 5 | 30 | | | | | |
| 6 | 40 | | | | | |
| 7 | 50 | | | | | |
| 8 | 10 | 3 | 18 | 4.5 | 4 | 7 |
| 9 | | 5 | | | | |
| 10 | | 10 | | | | |
| 11 | | 20 | | | | |
| 12 | | 30 | | | | |
| 13 | | 50 | | | | |
| 14 | | 80 | | | | |
| 15 | 10 | 10 | 2 | 4.5 | 4 | 7 |
| 16 | | | 8 | | | |
| 17 | | | 12 | | | |
| 18 | | | 18 | | | |
| 19 | | | 22 | | | |
| 20 | | | 30 | | | |
| 21 | | | 40 | | | |
| 22 | 10 | 10 | 18 | 2 | 4 | 7 |
| 23 | | | | 4.5 | | |
| 24 | | | | 8 | | |
| 25 | | | | 12 | | |
| 26 | | | | 20 | | |
| 27 | | | | 30 | | |
| 28 | | | | 50 | | |
| 29 | 10 | 10 | 18 | 4.5 | 2 | 7 |
| 30 | | | | | 4 | |
| 31 | | | | | 8 | |
| 32 | | | | | 15 | |
| 33 | | | | | 25 | |
| 34 | | | | | 35 | |
| 35 | | | | | 50 | |
| 36 | 10 | 10 | 18 | 4.5 | 4 | 3 |
| 37 | | | | | | 5 |
| 38 | | | | | | 7 |
| 39 | | | | | | 9 |
| 40 | | | | | | 11 |
| 41 | | | | | | 13 |
| 42 | | | | | | 15 |

In the numerical simulations, the effects of buried depth on the calculating results are carried out by adjusting the vertical principal stress σ_v . The corresponding σ_v of buried depths with 700, 900, 1100 and 1300 m are calculated by the parameters in Table 1 and equal to 10.98, 16.46, 21.95 and 27.44MPa, respectively.



(a) SR factor = 1.0

FLAC3D 3.00
 Step 8161 Model Perspective
 21:03:54 Sun Nov 06 2011

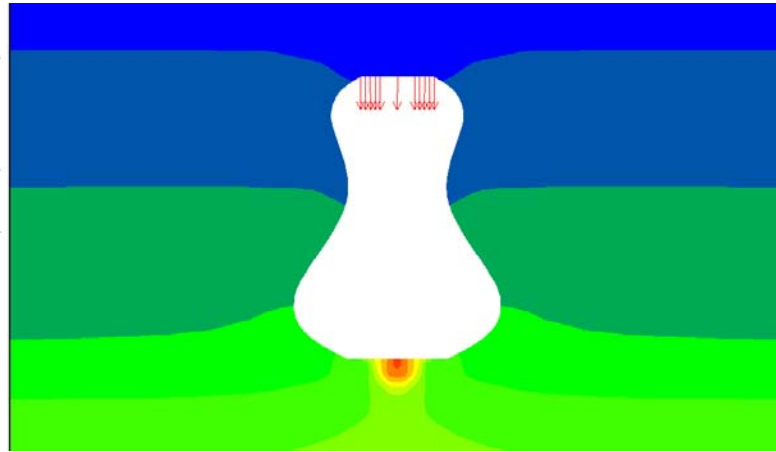
| | |
|------------------|--------------|
| Center: | Rotation: |
| X: 0.000e+000 | X: 0.000 |
| Y: 1.100e+002 | Y: 0.000 |
| Z: 5.885e+001 | Z: 0.000 |
| Dist: 1.493e+003 | Mag.: 3.05 |
| Increments: | Ang.: 22.500 |
| Move: 3.978e-002 | |
| Rot.: 10.000 | |

| | |
|---------------|---------------|
| Plane Origin: | Plane Normal: |
| X: 0.000e+000 | X: 0.000e+000 |
| Y: 1.000e-001 | Y: 1.000e+000 |
| Z: 0.000e+000 | Z: 0.000e+000 |

Contour of Z-Displacement
 Plane: on
 Magfac = 0.000e+000

| | |
|---|------------------------------|
| █ | -2.9149e-001 to -2.7500e-001 |
| █ | -2.7500e-001 to -2.5000e-001 |
| █ | -2.5000e-001 to -2.2500e-001 |
| █ | -2.2500e-001 to -2.0000e-001 |
| █ | -2.0000e-001 to -1.7500e-001 |
| █ | -1.7500e-001 to -1.5000e-001 |
| █ | -1.5000e-001 to -1.2500e-001 |
| █ | -1.2500e-001 to -1.0000e-001 |
| █ | -1.0000e-001 to -7.5000e-002 |
| █ | -7.5000e-002 to -5.0000e-002 |
| █ | -5.0000e-002 to -3.4544e-002 |

Itasca Consulting Group, Inc.
 Minneapolis, MN USA



(b) SR factor = 1.5

FLAC3D 3.00
 Step 8753 Model Perspective
 21:04:59 Sun Nov 06 2011

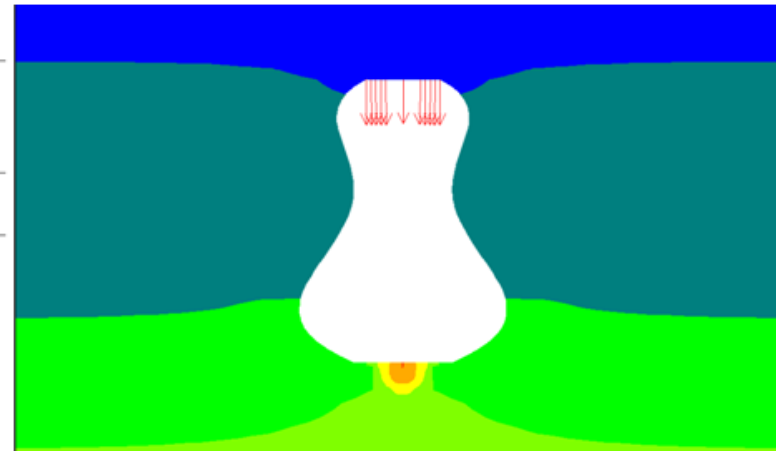
| | |
|------------------|--------------|
| Center: | Rotation: |
| X: 0.000e+000 | X: 0.000 |
| Y: 1.100e+002 | Y: 0.000 |
| Z: 5.885e+001 | Z: 0.000 |
| Dist: 1.493e+003 | Mag.: 3.05 |
| Increments: | Ang.: 22.500 |
| Move: 3.978e-002 | |
| Rot.: 10.000 | |

| | |
|---------------|---------------|
| Plane Origin: | Plane Normal: |
| X: 0.000e+000 | X: 0.000e+000 |
| Y: 1.000e-001 | Y: 1.000e+000 |
| Z: 0.000e+000 | Z: 0.000e+000 |

Contour of Z-Displacement
 Plane: on
 Magfac = 0.000e+000

| | |
|---|------------------------------|
| █ | -3.2105e-001 to -3.0000e-001 |
| █ | -3.0000e-001 to -2.5000e-001 |
| █ | -2.5000e-001 to -2.0000e-001 |
| █ | -2.0000e-001 to -1.5000e-001 |
| █ | -1.5000e-001 to -1.0000e-001 |
| █ | -1.0000e-001 to -5.0000e-002 |
| █ | -5.0000e-002 to -4.4978e-002 |

Interval = 5.0e-002
Displacement
 Plane: front
 Itasca Consulting Group, Inc.
 Minneapolis, MN USA



(c) SR factor = 2.0

FLAC3D 3.00
 Step 8366 Model Perspective
 21:05:47 Sun Nov 06 2011

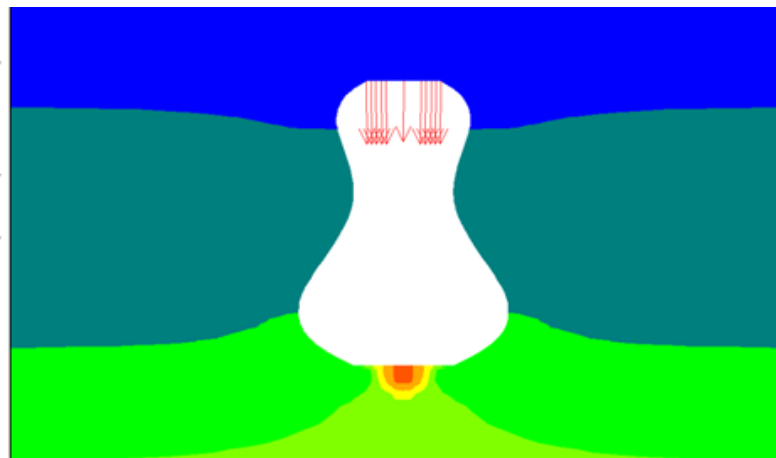
| | |
|------------------|--------------|
| Center: | Rotation: |
| X: 0.000e+000 | X: 0.000 |
| Y: 1.100e+002 | Y: 0.000 |
| Z: 5.885e+001 | Z: 0.000 |
| Dist: 1.493e+003 | Mag.: 3.05 |
| Increments: | Ang.: 22.500 |
| Move: 3.978e-002 | |
| Rot.: 10.000 | |

| | |
|---------------|---------------|
| Plane Origin: | Plane Normal: |
| X: 0.000e+000 | X: 0.000e+000 |
| Y: 1.000e-001 | Y: 1.000e+000 |
| Z: 0.000e+000 | Z: 0.000e+000 |

Contour of Z-Displacement
 Plane: on
 Magfac = 0.000e+000

| | |
|---|------------------------------|
| █ | -3.2972e-001 to -3.0000e-001 |
| █ | -3.0000e-001 to -2.5000e-001 |
| █ | -2.5000e-001 to -2.0000e-001 |
| █ | -2.0000e-001 to -1.5000e-001 |
| █ | -1.5000e-001 to -1.0000e-001 |
| █ | -1.0000e-001 to -5.0000e-002 |
| █ | -5.0000e-002 to -5.6717e-003 |

Interval = 5.0e-002
Displacement
 Plane: front
 Itasca Consulting Group, Inc.
 Minneapolis, MN USA



(d) SR factor = 2.5

Fig. 4: Vertical deformation contours of bedded rock salt cavern roof for SR factors with different values

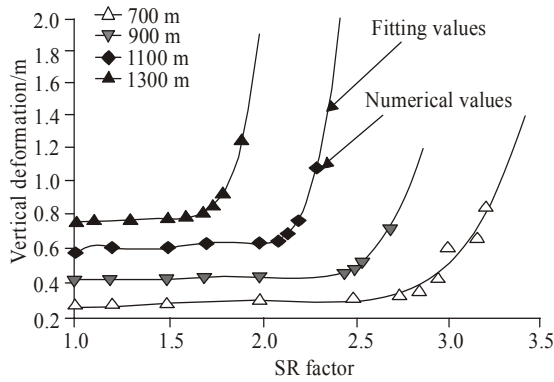


Fig. 5: Relations between the max. vertical deformations of cavern roof and SR factors under different buried depths

deformations and SR factors (Fig. 5) from numerical results. As shown in Fig. 5, the max. vertical deformations increase smoothly with the increase of SR factors when the SR factors are relative small. However, when the SR factors exceed certain critical values, the max. Vertical deformations significantly increase with a slight increase of SR factors. With the buried depth of 700 m and calculating condition of no. 2 (Table 2), the fifth-order polynomial formula between the max. vertical deformations and seven SR factors, arranging from 1.0 to 2.85, is obtained as:

$$z = -0.3081 + 1.7903F - 2.1678F^2 + 1.2796F^3 - 0.3648F^4 + 0.0404F^5 \quad (13)$$

According to (5), (6) and (13), the standard form of the potential function of deformations can be got:

$$V = \frac{1}{4}r^4 + \frac{1}{2}(-1.5765)r^2 + 0.7649r \quad (14)$$

Then, we get the control variables $u = -1.4143$ and $v = 0.6534$. Substituting them into (9), we obtain $f = 0.21 > \text{zero}$, indicating the cavern roof is still stable.

Similarly, we obtain the fifth-order polynomial formula between the max. vertical deformations and eight SR factors, arranging from 1.0 to 2.95 and its potential function as follows:

$$z = -3.3368 + 11.0337F - 13.0439F^2 + 7.4530F^3 - 2.0585F^4 + 0.2206F^5 \quad (15)$$

$$V = \frac{1}{4}r^4 + \frac{1}{2}(-2.6525)r^2 + 1.6578r \quad (16)$$

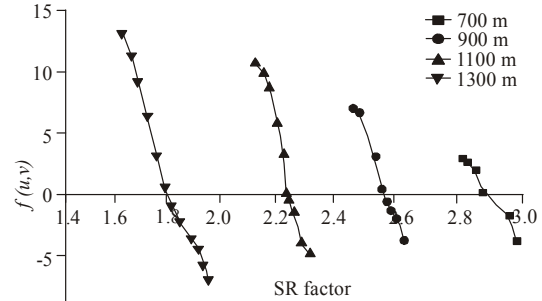


Fig. 6: Relations between the values of $f(u, v)$ and SR factors

According to (16), we get $u = -2.6525$ and $v = 1.6578$. Unfortunately, we obtain $f = -0.4453 < \text{zero}$, showing the cavern roof is failed.

From the above analyses, the critical stability factor of cavern roof with buried depth of 700 m and roof span of 10 m lies between 2.85 and 2.95. Taking safety side, the critical stability factor is proposed to be 2.85. If we want to improve the accuracy of roof stability factor, the SR factor F will be evaluated as 2.90 by the dichotomy method and repeating the above procedure. If $f > 0.0$, the critical stability factor lies between 2.85 and 2.90, otherwise it lies between 2.90 and 2.95. Then, the scope of critical stability factor is narrowed by repeating the procedure and ultimately the accuracy of cavern roof critical stability factor obtained by numerical simulations is improved. The traditional SR FEM could not achieve that. The catastrophic characteristic value $f(u, v)$ fluctuates severely at the close region of critical stability factor (Fig. 6), showing the failure of cavern roof is a typical process of deformation mutation and is accordance with the theory. The results also indicate the cusp catastrophe model used in assessing the stability factor of salt cavern roof is reasonable and approvable.

Similarly, the effects of buried depth, cavern roof span, roof salt thickness, roof salt stiffness, overlying non-salt thickness, overlying non-salt stiffness and gas pressure on the stability factors of salt cavern roof are obtained (Fig. 7). As shown in Fig. 7, the stability factors have inverse relationships with the buried depths. Because the loads subjected to the cavern roof increase progressively with the increase of buried depth, causing the decrease of cavern roof stability.

The correlations between the stability factors and cavern roof spans are plot in Fig. 7a. Caverns with larger roof spans have lower stability factors, as the cavern with large span will reduce the vertical component of stress at the salt cavern roof. The resulting increase in shear stress and decrease in mean

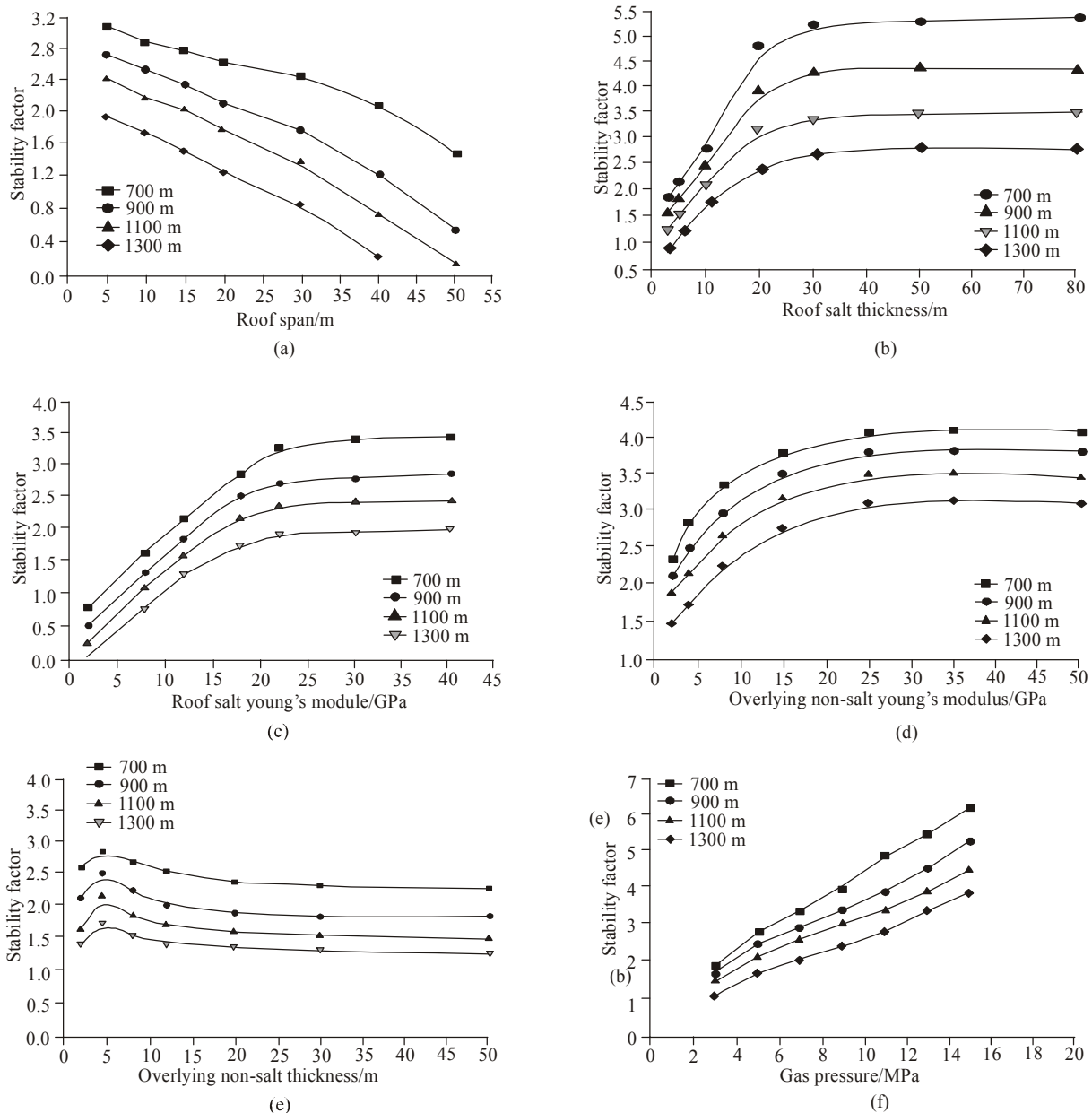


Fig. 7: Effects of influence parameters on the stability factors of cavern roof under different buried depths

stress can lead to shear failure of the salt. Ultimately, the vertical components of stress may become positive, which means that the rock above the cavern is then subjected to vertical tensions that may endanger the stability of cavern roof. Therefore, proper cavern roof span plays an important role in ensuring roof stability and increasing cavern volume.

Fig. 7b provides the effects of roof salt thicknesses on the roof stability factors. Roof salt thickness has great influences on the stability factor when it does not exceed 20 m. However, when the thickness exceeds 20

m, its influences become less notable for little load carrying capacity of roof salt left except self-weights. In the actual engineering, the roof salt can provide a barrier of rock having a low permeability necessary to prevent the upward migration of gas. So, a relative thick roof salt is suggested to maintain the salt cavern stability and sealing.

Figure 7c and d show the stability factors of cavern roof are equidirectional with the increase of Young's modulus of roof salt and overlying non-salt, as the increase of Young's modulus can enhance the load

capacity and stability of cavern roof. In addition, when the Young's modulus of overlying non-salt is less than about 10 GPa, it has bad effects on the cavern roof stability. Unfortunately, the Young's modulus of overlying non-salt (e.g., shale, anhydrite and glauberite, etc) is usually less than 10 GPa in most bedded rock salt formation. Therefore, the thickness of roof salt is one of the key factors to be considered in design and construction of bedded rock salt cavern to prevent cavern roof collapse.

As shown in Fig. 7e, the thickness of overlying non-salt has little influences on the stability factors of cavern roof because the non-salt has a low Young's modulus according to the experimental data. It makes the overlying non-salt has little load carrying capacity left except self-weight. The high gas pressure is beneficial to the stability of cavern roof (Fig. 7f) because it can balance part of the overburden loaded on the cavern roof. During the natural gas storage running, the time of salt cavern with low gas pressure should be reduced as shortly as possible to ensure the cavern roof stability.

CONCLUSION

- The cusp catastrophe model is proposed in the study to evaluate the stability factor of bedded rock salt cavern roof, which overcomes the shortages of traditional SR FEM that the failure criteria cannot be given precisely and improves the calculation accuracy of numerical simulations. Numerical simulations of the generic bedded rock salt caverns are used to illustrate the detailed procedures of the stability factor evaluated by the proposed model. Furthermore, the effects of several design parameters on the cavern roof stability are studied
- The numerical simulation examples show the cusp catastrophe model is efficient and precise in predicting the stability factor of bedded rock salt cavern roof. The mathematical and physical meanings of the model are very definite and easy to be understood. The model is versatile and can be widely used in other similar engineering fields
- The results show that the buried depth, roof span and gas pressure have significant effects on the roof stability and can be controlled in the designs and operations. Therefore, the proper buried depth, strictly designed cavern roof and short time of low gas pressure are recommended in the design of bedded rock salt cavern gas storage. As the stiffness and strength of non-salt are usually very low, a relative thick roof salt is recommended to maintain the cavern roof stability

ACKNOWLEDGMENT

The authors wish to acknowledge the financial support of China Postdoctoral Science Foundation funded project (No. 2012M511557) and Post-doctor Innovation Research Program of Shandong Province (No.201102033).

REFERENCES

- Borniyakov, S.A., V.A. Truskov and A.V. Cheremnykh, 2008. Dissipative structures in fault zones and their diagnostic criteria (from physical modeling data). *Russ. Geol. Geophys.*, 49(2): 138-143.
- Dawson, E., F. Motamed, S. Nesarajah and W. Roth, 2000. Geotechnical stability analysis by strength reduction. *Slope Stability, Proceeding of Sessions of Geo-Denver, Colorado*, pp: 99-113.
- Dawson, E., W.H. Roth and A. Drescher, 1999. Slope stability analysis by strength reduction. *Geotechnique*, 49(6): 835-840.
- Diederichs, M.S., M. Lato, R. Hammah and P. Quinn, 2007. Shear Strength Reduction (SSR) approach for slope stability analyses. *Proceedings of the 1st Canada-US Rock Mechanics Symposium, Vancouver, BC, Canada*, pp: 319-327.
- Donald, I.B. and S.K. Giam, 1988. Application of the nodal displacement method to slope stability analysis. *Proceedings of the 5th Australia-New Zealand Conference on Geomechanics, Sydney, Australia*, pp.456-460.
- Fu, C.H. and S.H. Chen, 2008. Study on instability criteria of surrounding rock of underground engineering cavern based on catastrophe theory. *Rock Soil Mech.*, 29(1): 167-172. (in Chinese).
- Griffiths, D.V. and P.A. Lane, 1999. Slope stability analysis by finite elements. *Geotechnique*, 49(3): 387-403.
- Huang, M.S. and C.Q. Jia, 2009. Strength reduction FEM in stability analysis of soil slopes subjected to transient unsaturated seepage. *Comput. Geotech.*, 36(1-2): 93-101.
- Joanna, L.G., R.M. Adrian and M.D. Cole, 2010. Strength reduction factors for near-fault forward-directivity ground motions. *Eng. Struct.*, 32(1): 273-285.
- Kemal, H., B.B. Hasan and B. Alemdar, 2007. Nonlinear analysis of rock-fill dams to non-stationary excitation by the stochastic Wilson- θ method. *Appl. Math. Comput.*, 194(2): 333-345.
- Leynaud, D. and N. Sultan, 2010. 3-D slope stability analysis: A probability approach applied to the nice slope (SE France). *Mar. Geol.*, 269(3-4): 89-106.

- Liang, W.C., Y. Yang, M.B. Zhao and M.B. Dusseault, 2007. Liu J. Experimental investigation of mechanical properties of bedded salt rock. *Int. J. Rock Mech. Min. Sci.*, 44(3): 400-411.
- Manzari, M.T. and M.A. Nour, 2000. Significance of soil dilatancy in slope stability analysis. *J. Geotech. Geoenviron. Eng.*, 126(1): 75-80.
- Matsui, T. and K.C. San, 1992. Finite element slope stability analysis by shear strength reduction technique. *Soils Foundat.*, 32(1): 59-70.
- Qin, S.Q., J.J. Jiao and S.J. Wang, 2001. A nonlinear catastrophe model of instability of planar-slip slope and chaotic dynamical mechanisms of its evolutionary process. *Int. J. Solids Struct.*, 38(44-45): 8093-8109.
- Sanavia, L., 2009. Numerical modeling of a slope stability test by means of porous media mechanics. *Eng. Comput.*, 26(3): 245-266.
- Thom, R., 1989. *Structural Stability and Morphogenesis: An Outline of a General Theory of Models*. 2nd Edn., Addison-Wesley, Reading, pp: 348, ISBN: 0201094193.
- Ugai, K. and D. Leshchinsky, 1995. Three-dimensional limit equilibrium and finite element analysis: A comparison of results. *Soils Foundat.*, 35(4): 1-7.
- Ugai, K., 1989. A method of calculation of total factor of safety of slopes by elasto-plastic FEM. *Soils Foundat.*, 29(2): 190-195.
- Vries, D.K., 2006. Improved modeling of bedded salt cavern stability. *GASTIPS*, 12(1): 15-17.
- Wang, T.T., X.Z. Yan, H.L. Yang and X.J. Yang, 2011a. Stability analysis of the pillars between bedded salt cavern groups by cusp catastrophe model. *Sci. China Technol. Sci.*, 54(6): 1615-1623.
- Wang, T.T., X.Z. Yan, H.L. Yang and X.J. Yang, 2011b. Stability analysis of pillars between bedded salt cavern gas storages. *J. China Coal Soc.*, 36(5): 790-795.
- Wang, T.T., X.Z. Yan, X.J. Yang and H.L. Yang, 2010a. Surface dynamic subsidence prediction above salt cavern gas storage considering the creep of rock salt. *Sci. China Technol. Sci.*, 53: 3197-3202.
- Wang, T.T., X.Z. Yan, X.J. Yang and H.L. Yang, 2010b. Improved Mohr-Coulomb criterion applicable to gas storage caverns in multilaminated salt stratum. *Acta Petrolei Sinica*, 31(6): 1040-1044.
- Wei, W.B. and Y.M. Cheng, 2009. Strength reduction analysis for slope reinforced with one row of piles. *Comput. Geotech.*, 36(7): 1176-1185.
- Xu, C.H. and Q.W. Pen, 2004. Criterion of entropy catastrophe of stability of surrounding rock. *Rock Soil Mech.*, 25(3): 34-40. (in Chinese).
- Yang, C.H., Y.P. Li and D.A. Qu, 2008. Advances in researches of the mechanical behaviors of bedded salt rocks. *Adv. Mech.*, 38(4): 484-494. (in Chinese).
- Yang, K., T.X. Wang and Z.T. Ma, 2010. Application of cusp catastrophe theory to reliability analysis of slopes in open-pit mines. *Min. Science Technol.*, 20(1): 71-75.
- Zhou, C.Y., H. Chen and F.X. Zhu, 2008. Research on nonlinear dynamic warning for high slopes based on progressive evolution process. *Chinese J. Rock Mech. Eng.*, 27(4): 818-824. (in Chinese).
- Zienkiewicz, O.C., C. Humpheson and R.W. Lewis, 1975. Associated and non-associated viscoplasticity and plasticity in soil mechanics. *Geotechnique*, 25(4): 671-689.